Appl. Math. Mech. -Engl. Ed., **32**(4), 437–448 (2011)
DOI 10.1007/s10483-011-1428-7
©Shanghai University and Springer-Verlag
Berlin Heidelberg 2011

Applied Mathematics and Mechanics (English Edition)

Simulation of tumor microvasculature and microenvironment response to anti-angiogenic treatment by angiostatin and endostatin*

Jie WU (吴　洁)[1],　Zu-rong DING (丁祖荣)[1],　Yan CAI (蔡　彦)[2],
Shi-xiong XU (许世雄)[2],　Gai-ping ZHAO (赵改平)[3],　Quan LONG (龙　泉)[4]

(1. School of Naval Architecture, Ocean and Civil Engineering, Shanghai Jiaotong University, Shanghai 200240, P. R. China;
2. Department of Mechanics and Engineering Science, Fudan University, Shanghai 200433, P. R. China;
3. School of Medical Instrument and Food Engineering, University of Shanghai for Science and Technology, Shanghai 200093, P. R. China;
4. Brunel Institute for Bioengineering, Brunel University, Uxbridge, Middlesex, UK)

Abstract The effects of anti-angiogenesis treatment by angiostatin and endostatin on normalization of tumor microvasculature and microenvironment are investigated, based on mathematical modeling and numerical simulation of tumor anti-angiogenesis and tumor haemodynamics. The results show that after anti-angiogenesis treatment: (i) the proliferation, growth, and branching of neo-vessels are effectively inhibited, and the extent of vascularization in tumors is accordingly reduced. (ii) the overall blood perfusion inside of tumor is declined, the plateau of tumor interstitial fluid pressure (IFP) is relieved, the interstitial fluid oozing out from the tumor periphery into the surrounding normal tissue is reduced, the reduction of overall extravasation across vasculature to tumor interstium is much less than the decreased overall blood perfusion, due to the decline of IFP, the intravasations is remarkablely effected by the change, in some cases there are no intravasation flow appear.

Key words solid tumor, microenvironment normalization, numerical simulation, anti-angiogenesis

Chinese Library Classification R318.01, TB115
2010 Mathematics Subject Classification 92C10, 92C15

1 Introduction

Unlike the normal blood vessels, tumor vasculature has abnormal organization, structure, and function. Tumor vessels are leaky and blood flow is heterogeneous and often compromised. Vascular hyperpermeability and the lack of functional lymphatic vessels inside tumors

* Received May 7, 2010 / Revised Feb. 23, 2011
Project supported by the National Natural Science Foundation of China (No. 10772051) and the Postdoctral Foundation of China (No. 20100470702)
Corresponding author Jie WU, Ph. D., E-mail: janny_wujie@yahoo.com.cn

cause elevation of interstitial fluid pressure (IFP) in solid tumors[1]. These characteristics cause abnormal microenvironment in tumors and form a physiological barrier to the delivery of therapeutic agents to tumors. Furthermore, elevated tumor IFP increases fluid flow from the tumor margin into the peri-tumor area and may facilitate peri-tumor lymphatic hyperplasia and metastasis[1–2].

Tumor vasculature is not a simple supply line of nutrients to tumors. It governs pathophysiology of solid tumors and thus, tumor growth, invasion, metastasis, and response to various therapies. Anti-angiogenic treatments directly targeting angiogenic signaling pathways as well as indirectly modulating angiogenesis show normalization of tumor vasculature and microenvironment at least transiently in both preclinical and clinical settings[1,3–6]. Endostatin (ES) has been considered as one of the most potential anti-angiogenic drugs. It can inhibit endothelial cell proliferation, migration, invasion, and tube formation[7]. Angiostatin (AS), one of anti-angiogenic factors, can induce tumor dormancy by inhibiting endothelial cell proliferation[8]. While these anti-angiogenic drugs have been approved for cancer treatment, it appears that the clinical application of the agents on anti-angiogenic therapy is more complex than originally thought.

Due to the scale of tumor microvessel, little is known about how vasculature structure and microenvironmental flow is affected by anti-angiogenesis therapy, even with the current state of the art imaging techniques. Therefore, numerical simulation could be an effective study method. There are a few mathematical models of tumor anti-angiogenesis have been developed so far[9–10]. However, none of them were used to further investigate the normalization of tumor microenvironment by anti-angiogenesis. The purpose of this paper is to investigate the effects of anti-angiogenesis treatments (by AS and ES) on tumor microvasculature and resultant microenvironment normalization. Figure 1 describes the major structure of the study. It is based on two mathematical models: (a) tumor anti-angiogenesis and (b) tumor haemodynamics.

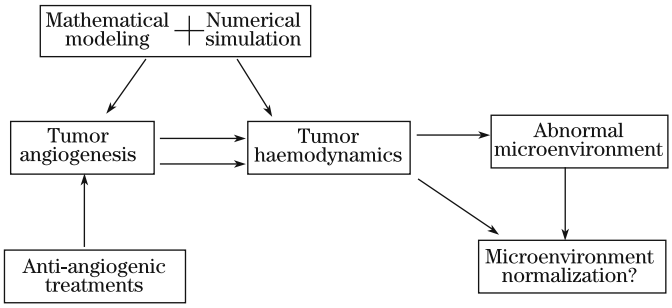

Fig. 1 Structure of the study

2 Models and methods

2.1 Model of tumor anti-angiogenesis

The factors that influencing tumor angiogenesis activities included in the present model are the proliferation of endothelial cells (ECs), the migration of EC through random motility, chemotaxis in response to tumor angiogenesis factors (AGF) released by the tumor, and haptotaxis in response to fibronectin (FN) gradients in the excellular matrix (ECM). In addition, the inhibition of AS and ES on EC proliferation and apoptosis are also considered. The density of ECs n, the AGF concentration c, the FN concentration f, the AS concentration a, and the

ES concentration in plasma e, satisfy the following non-dimensional equations[9–11],

$$\begin{cases} \dfrac{\partial n}{\partial t} = D\nabla^2 n - \nabla\cdot\Big(\dfrac{\chi}{1+\sigma c}n\nabla c\Big) - \nabla\cdot(\xi a n\nabla a) - \nabla\cdot(\rho n\nabla f) \\ \qquad\quad + \beta_{\mathrm{r}}(1-n)nH(c)\Big(1-\dfrac{\varepsilon_{\max}ee_0}{eC_{50}+ee_0}\Big) - \beta_{\mathrm{d}}n, \\ \dfrac{\partial f}{\partial t} = \beta n - \gamma n f, \\ \dfrac{\partial c}{\partial t} = -\eta n c, \\ \dfrac{\partial a}{\partial t} = D_{\mathrm{a}}\dfrac{\partial a^2}{\partial^2 x} - \gamma_{\mathrm{a}}a, \\ \dfrac{\partial e}{\partial t} = -\gamma_{\mathrm{c}}e + \gamma_{\mathrm{u}}U_{\mathrm{I,ex}}, \end{cases} \tag{1}$$

where D, χ, and ρ are the coefficients of EC diffusion, chemotaxis to AGF, and haptotaxis to ECM, respectively. ξ is the EC chemotaxis coefficient to AS. β_{r} is the EC proliferation rate. $H(c)$ is an on-off function,

$$H(c) = \begin{cases} 0, & c \leqslant c^*, \\ c - c^*, & c > c^*. \end{cases}$$

It means that if c is higher than a threshold value c^*, the EC may proliferate, otherwise it stays dormancy, $\varepsilon_{\max}$ is the maximum inhibiting effect of endostatin on ECs, eC_{50} is ES concentration that induce 50% of the maximum inhibiting effect, e_0 is the initial concentration of ES, β_{d} is EC loss rate. β is FN production rate, γ is FN rate of uptake by ECs. η is AGF rate of uptake by ECs, D_{a} is AS diffusion coefficient, γ_{a} is AS rate of uptake by ECs, γ_{c} is ES plasma clearance rate, $U_{\mathrm{I,ex}}$ is the exogenous input of ES, and γ_{u} is the positive coefficient of ES input. The values of these parameters can be found in [9–10].

The simulation space is a 2D domain with a size of 4 mm×4 mm, as shown in Fig. 2. Two parent vessels are located on the left and right boundaries, a small tumor with a radius (R_{t}) of 1 mm is at the center and surrounded by the normal tissues of the host. 2D9P simulation scheme is used in this paper, please see the detail in [12].

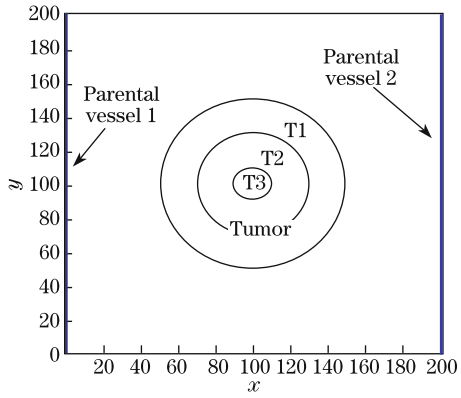

Fig. 2 2D tumor anti-angiogenesis model scheme

2.2 Model of tumor haemodynamics

The flow model is used based on our previous work[12–13], which couples (a) intravascular blood flow, (b) transvascular leakiness, (c) interstitial fluid movement, (d) blood rheology, (e) vessel compliance, and (f) lymphatic absorption.

2.2.1 Intravascular blood flow

Assume flux conservation and incompressible flow at each node o,

$$\sum_{k=1}^{8} Q_o^k B_o^k = 0, \tag{2}$$

$$Q_o^k = Q_{\mathrm{V},o}^k - Q_{\mathrm{t},o}^k, \tag{3}$$

where B_o^k=1 (or B_o^k=0) is a positive (or negative) integer representing the connectivity between node o and its adjacent node k, Q_o^k is the flowrate from node k to node o (see Fig. 3), $Q_{\mathrm{V},o}^k$ is the intravascular flowrate without fluid leakage, described by local Poiseuille's law,

$$Q_{\mathrm{V},o}^k = \frac{\pi R_k^4}{8\mu_k} \frac{(P_{\mathrm{V},k} - P_{\mathrm{V},o})}{\Delta l_k}, \tag{4}$$

and $Q_{\mathrm{t},o}^k$ is the transvascular flowrate, following Starling's law,

$$Q_{\mathrm{t},o}^k = 2\pi R_k \Delta l_k L_{\mathrm{pV}} (\overline{P}_{\mathrm{V},o}^k - \overline{P}_{\mathrm{i},o}^k - \sigma_{\mathrm{T}}(\pi_{\mathrm{V}} - \pi_{\mathrm{i}})), \tag{5}$$

where $P_{\mathrm{V},o}$ and $P_{\mathrm{V},k}$ are the intravascular pressure of node o and k, $\overline{P}_{\mathrm{V},o}^k$ is the mean intravascular pressure in vascular element k, $\overline{P}_{\mathrm{i},o}^k$ is the mean interstitial pressure outside vascular element k, μ_k is the blood viscosity in vascular element k, Δl_k and R_k are the length and radius of vascular element k,

$$\Delta l_k = \begin{cases} \Delta l & (k = 1, 2, 3, 4), \\ \sqrt{2}\Delta l & (k = 5, 6, 7, 8), \end{cases}$$

L_{pV} is the hydraulic permeability of blood vessel wall, σ_{T} is the average osmotic reflection coefficient for plasma proteins, and π_{V} and π_{i} are the colloid osmotic pressures of plasma and interstitial fluid.

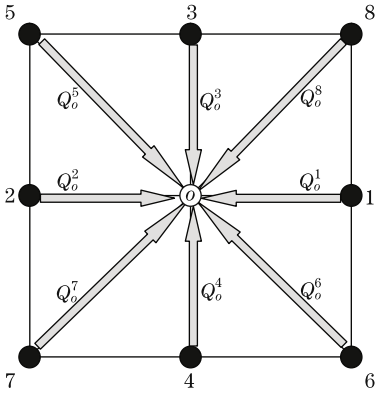

Fig. 3 Schematic representation of blood flux at each vascular node

2.2.2 Interstitial fluid flow

The interstitial fluid flow is modeled by Darcy's law,

$$U_{\mathrm{i}} = -K\nabla P_{\mathrm{i}}, \tag{6}$$

where U_{i} is the interstitial fluid velocity, and K is the hydraulic conductivity coefficient of the interstitium.

The equation of interstitial pressure P_{i} is described by[13]

$$\nabla^2 P_{\mathrm{i}} = \frac{L_{\mathrm{pV}} S_{\mathrm{V}}}{KV}(P_{\mathrm{i}} - P_{\mathrm{eV}}) + \frac{L_{\mathrm{pL}} S_L}{KV}(P_{\mathrm{i}} - P_{\mathrm{eL}})H(P_{\mathrm{i}}), \tag{7}$$

where L_{pV} is the hydraulic permeability of blood vessel wall, L_{pL} is the hydraulic permeability of lymphatic vessel wall, $S_{\mathrm{V}}/V = \sum\limits_k \pi R_k/\Delta l_k^2$ is the surface area of blood vessel wall per unit volume of tissue, and S_{L}/V is the surface area of lymphatic vessel wall per unit volume of tissue. Here, $L_{\mathrm{pL}}S_{\mathrm{L}}/V$ is assumed to be zero for tumor tissue, and given a uniform value for normal tissue referring to [14]. $P_{\mathrm{eV}} = P_{\mathrm{V}} - \sigma_{\mathrm{T}}(\pi_{\mathrm{V}} - \pi_{\mathrm{i}})$ is the effective pressure inside blood vessels, and P_{eL} is the effective pressure inside lymphatic vessels.

$$H(P_{\mathrm{i}}) = \begin{cases} 1, & P_{\mathrm{i}} \geqslant P_{\mathrm{eL}}, \\ 0, & P_{\mathrm{i}} < P_{\mathrm{eL}}, \end{cases}$$

representing that no fluid in the lymphatic vessels would filtrate into the interstitium, even if the interstitial pressure is below the lymphatic pressure[15].

The continuity of pressure and flux on the interconnected boundary between the tumor and normal tissue Γ are as follows:

$$\begin{cases} P_{\mathrm{i}}|_{\Gamma^-} = P_{\mathrm{i}}|_{\Gamma^+}, \\ -K_{\mathrm{T}}\nabla P_{\mathrm{i}}|_{\Gamma^-} = -K_{\mathrm{N}}\nabla P_{\mathrm{i}}|_{\Gamma^+}, \end{cases} \tag{8}$$

K_{N} and K_{T} are the hydraulic conductivity coefficients of normal tissue and tumor tissue, respectively.

2.2.3 Vessel compliance

It is assumed the blood vessels outside tumor are rigid, while the intra-tumoral ones are compliant specified by a equation first proposed by Netti[16],

$$R = R_{\mathrm{ini}}\Big(\frac{P_{\mathrm{V}} - P_{\mathrm{i}} + P_{\mathrm{c}}}{E}\Big)^b, \tag{9}$$

where R is the vessel radius, R_{ini} is the initial radius obtained from the angiogenesis simulation, b is the compliance exponent, E is the compliance coefficient, and P_{c} is the collapse pressure.

2.2.4 Blood rheology

The formula developed by Pries et al.[17] is adopted to describe viscosity changes,

$$\begin{cases} \mu = \mu_{\mathrm{pla}}\Big(1 + (\mu_{0.45} - 1)\dfrac{(1-H)^c - 1}{(1-0.45)^c - 1}\Big(\dfrac{2R}{2R-1.1}\Big)^2\Big)\Big(\dfrac{2R}{2R-1.1}\Big)^2, \\ \mu_{0.45} = 6\mathrm{e}^{-0.17R} + 3.2 - 2.44\mathrm{e}^{-0.06(2R)^{0.645}}, \\ c = (0.8 + \mathrm{e}^{-0.15R})\Big(-1 + \dfrac{1}{1 + 10^{-11}(2R)^{12}}\Big) + \dfrac{1}{1 + 10^{-11}(2R)^{12}}, \end{cases} \tag{10}$$

where μ_{pla} is the viscosity of plasma, and H is the blood hematocrit.

The distribution of red blood cells (RBCs) at microvascular bifurcations is represented according to the approach proposed by Pries et al.[18]. The fractional flow of erythrocytes into one daughter branch ($Q_{\mathrm{F,E}}$) is calculated from the respective fractional blood flow ($Q_{\mathrm{F,B}}$) as follows:

$$\begin{cases} \mathrm{logit}(Q_{\mathrm{F,E}}) = \Phi_1 + \Phi_2 \mathrm{logit}\Big(\dfrac{Q_{\mathrm{F,B}} - \Phi_3}{1 - 2\Phi_3}\Big), \\ \Phi_1 = -13.29 \dfrac{d_\alpha^2/d_\beta^2 - 1}{d_\alpha^2/d_\beta^2 + 1} \dfrac{1 - H_{\mathrm{m}}}{d_{\mathrm{m}}}, \\ \Phi_2 = 1 + 6.98 \dfrac{1 - H_{\mathrm{m}}}{d_{\mathrm{m}}}, \\ \Phi_3 = 0.964 \dfrac{1 - H_{\mathrm{m}}}{d_{\mathrm{m}}}, \end{cases} \tag{11}$$

where logit x=ln$(x/(1-x))$. Parameter Φ_1 describes the difference between the relations derived for the two daughter branches, Φ_2 denotes the nonlinearity of the relation between $Q_{\mathrm{F,E}}$ and $Q_{\mathrm{F,B}}$, and Φ_3 defines the minimal fractional blood flow required to draw RBCs into the daughter branch. d_α, d_β, and d_{m} are the diameters of the daughter branches and the mother vessel, H_{m} is the discharge hematocrit in the mother vessel. In these relations, all diameters are given in micrometers.

3 Simulation results

3.1 Tumor anti-angiogenic microvasculature

In this paper, four different cases were generated based on the different chemotaxis factors. They are, (i) AGF—AGF is the only chemotaxis factor; (ii) AGF&AS—AGF and AS are the chemotaxis factors; (iii) AGF&ES—both AGF and ES are the chemotaxis factors with an ES infusion of 20 mg/(kg·d); and (iv) AGF&AS&ES:10, AGF&AS&ES:6, AGF&AS&ES:4—the chemotaxis factors are AGF, AS, and an ES infusion of 20 mg/(kg·d) since the 10th, 6th, and 4th day from angiogenesis start, respectively. The results of AGF only case is taken as the control group, while the other five are considered the study groups.

Figure 4 shows the microvascular networks from the anti-angigenesis simulations. Figure 4(a) is the result of AGF case. The network presents the abnormal geometric and morphological features of tumor microvasculature, such as vessel tortuosity, heterogeneous density distribution, "brush border" phenomenon. The extensive neovessel bed can supply not only the nutrients for the rapid growth of tumor tissues, but also the metastasis pathways for tumor cells. The result of AGF&AS case is shown in Fig. 4(b). Under the inhibition effects of AS, the angiogenic network has become sparser with decreased vessel density, while the growth rate of the capillary sprouts have not been inhibited potently. Figure 4(c) shows the result of AGF&ES case, compared with Fig. 4(a), the growth rate and the vessel branching decreased with a reduced vessel density under the inhibiting effects of ES. Figures 4(d) – 4(f) represent the networks simulated of AGF&AS&ES cases. The figures show that the growth, proliferation, and branching of new vessels are distinctly inhibited, and the extents of vascularization are greatly decreased. Moreover, the earlier ES infusion, the better inhibition effects. Particularly in Fig. 4(e) and Fig. 4(f), although a part of sprouts have grown into the tumor, the vessel networks have not matured to supply nutrients for the further development and pathways for the metabolic wastes because of the significant reduction of blood vessel density.

Also, we introduce microvessel density (MVD) to compare the anti-angiogenesis effects of AS and ES quantitatively. Due to the simulation randomicities, 50 simulations are carried out for each case to obtain the average MVD, as shown in Fig. 5. According to the figure, both single and combination effects of AS and ES can effectively inhibit the process of tumor angiogenesis, especially for the combined model at an earlier stage (e.g., AGF&AS&ES:6 and

AGF&AS&ES:4). The experimental results in which human dermal microvascular endothelial cells (HDMECs) were cultured, showed that the number of microvessels decreased after using AS and ES[19], which is well shown in our simulation results.

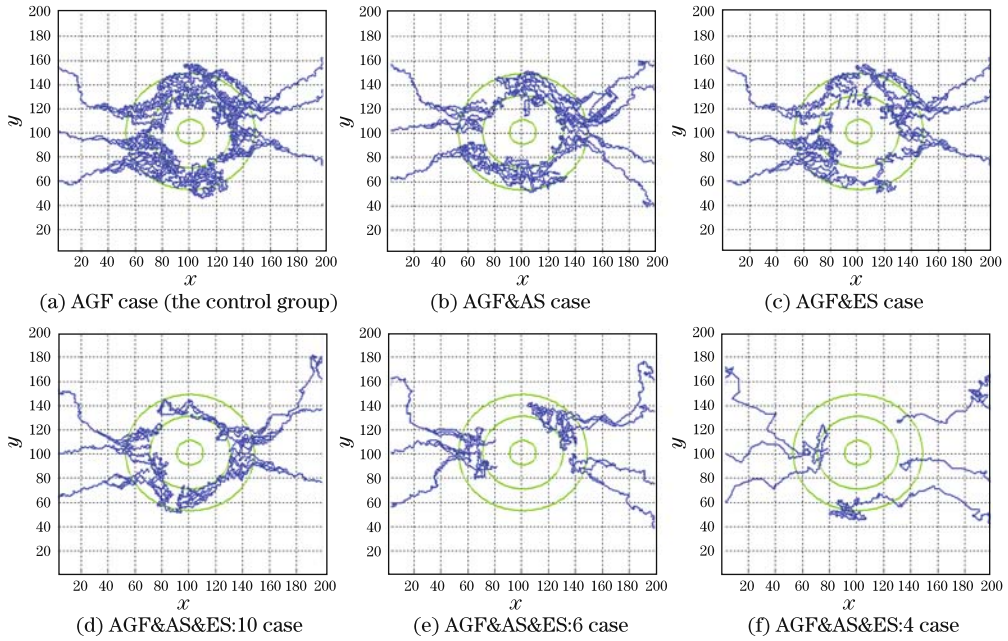

Fig. 4 Microvascular networks from the anti-angiogenesis simulations

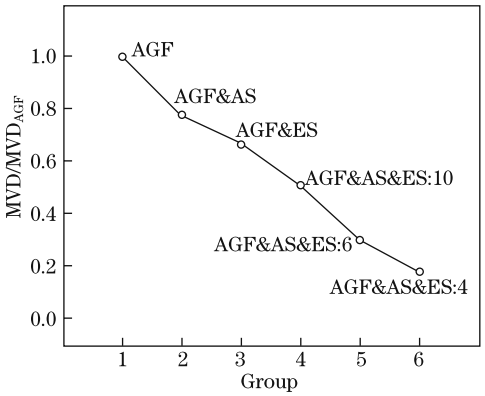

Fig. 5 Comparison of MVD values of the six groups

3.2 Tumor haemodynamics on anti-angigenic microvasculature

The parameter values are listed in Table 1. The inlet and outlet pressure of the two parent vessels are given $P_{\text{in},1} = P_{\text{in},2} = 25$ mmHg, $P_{\text{out},1} = P_{\text{out},2} = 10$ mmHg.

3.2.1 Flows on the vasculature without anti-angiogenesis treatment (AGF case)

Figure 6 shows the flow simulation results on the AGF vascular network in Fig. 4(a) (the control one). Figures 6(a) – 6(d) are the distributions of intravascular pressure P_{V}, intravascular velocity U_{V}, transvascular velocity U_{t}, interstitial pressure P_{i} and interstitial velocity U_{i}, respectively. The results predict the abnormal microcirculation and the resultant hostile microenvironment of tumors, such as poor blood perfusion, large amount of vascular leakiness, elevated interstitial fluid pressure, extremely slow interstitial flow inside tumor and a rapidly

rising convection oozing out from tumor margin into surrounding host tissue, all of which consisted with the corresponding experimental observations reported[1]. These features create a great barrier for drug delivery in tumor therapies.

Table 1 Parameter values used in flow simulations

Parameter	Value	Parameter	Value
L_{pV}/ (cm/(mmHg·s))[1]	Normal: 3.6×10^{-8} Tumor: 1.86×10^{-6}	$\frac{L_{\mathrm{pL}}S_{\mathrm{L}}}{V}$/ (1/(mmHg·s))*	Normal: 1.0×10^{-4} Tumor: 0
K/(cm^2/(mmHg·s))[1]	Normal: 2.5×10^{-7} Tumor: 2.5×10^{-7}	σ_{T}[1]	Normal: 0.91 Tumor: 8.7×10^{-5}
π_{V}/mmHg[1]	Normal: 20 Tumor: 19.8	π_{i}/mmHg[1]	Normal: 10 Tumor: 17.3
P_{eL}/ mmHg*	Normal: 0.5	P_{c} / mmHg[16]	3.0
b[16]	0.1	E / mmHg[16]	6.5

*estimated according to the physiological values.

3.2.2 Comparisons of the flows on the vasculature with and without anti-angiogensis treatments

Likewise, we used the flow values of AGF case as the control group, and made comparisons with the corresponding results obtained from the other five groups (AGF&AS, AGF&ES, AGF&AS&ES:10, AGF&AS&ES:6, AGF&AS&ES:4). In Fig. 7, each data is the average flow value based on 50 simulated networks of the corresponding anti-angiogenesis cases to provide a general trend of the flows.

Figure 7(a) shows the comparison of the overall blood perfusion through the vasculature, $Q_{\mathrm{V}}/Q_{\mathrm{V(AGF)}}$. Q_{V} of the groups AGF&ES, AGF&AS&ES:10, AGF&AS&ES:6, AGF&AS&ES:4 decrease about 16%, 33%, 55%, and 65%, respectively, while the value of AGF&AS group is close to the control one $Q_{\mathrm{V(AGF)}}$. Herbst et al.[20] have studied the effects of ES on tumors (as anti-angiogensis therapy) by clinical trails. The results predicted that tumor blood flow reduced 20% after the first treatment cycle. Our result (see Fig. 7(a)) is at the similar range to it. Other clinical researches also indicated that anti-angiogenesis therapy can cut down blood flow inside of tumors, e.g., Willett et al.[5–6] found nearly 30% decrease of tumor blood perfusion determined by functional CT after the anti-angiogensis treamtment using bevacizumab.

Interstitial hypertension is a reflection of the global pathophysiology of solid tumors and may be used for diagnosis, prognosis, and/or monitoring of treatment responses[2]. Figure 7(b) shows the comparison of the interstitial pressure P_{i} (i.e., IFP) in the tumor center. Compared with the control group, P_{i} in the groups of AGF&AS, AGF&ES, AGF&AS&ES:10, AGF&AS&ES:6, AGF&AS&ES:4 declined about 17%, 20%, 47%, 60%, and 60%, respectively, indicating the IFP plateau is effectively relieved. Accordingly, the velocity of the interstitial fluid at tumor margin decline by 9%, 12%, 23%, 34%, and 37%, (see Fig. 7(c)). It reduces the convective flow out of the tumor and may also enhance drug residential time within the tumor. Data obtained in recent clinical trials also support the above results. IFP measured by a wick-in-needle technique showed a 70% drop in rectal carcinomas 12 days after infusion of bevacizumab in patients[5–6]. Agents such as Bevacizumab, DC101, and SU11657 decrease tumor IFP in breast, colon cancers, and gliomas[3–4].

The transvascular flux in tumors is as the same magnitude of the intravascular flux, which not only influences tumor microenvironment, but also provides a carrier for drug delivery and metastasis of tumor cells or growth factors of angiogenesis and lymphangiogenesis[1]. The comparison of the overall transvascular flow is shown in Fig. 7(d) and Fig. 7(e). The extravasation flow (outward flow from blood vessels) is defined as Q_{t}^{+} (see Fig. 7(d)), while the intravasation flow (inward flow) as Q_{t}^{-} (see Fig. 7(e)). Q_{t}^{+} increases about 15% and 12% in groups AGF&AS

and AGF&ES, close to the control value in AGF&AS&ES:10, and declines 14% and 16% in AGF&AS&ES:6, AGF&AS&ES:4. Q_{t}^{+} is helpful to drug delivery across vascular network to tumor intersitium. Therefore, the higher of Q_{t}^{+} the better of the tumor blood perfusion. Due to the greatly decreasing of overall blood perfusion of the study groups, especially in the last three (see Fig. 7(a)), Q_{t}^{+} reduces accordingly which is only a small amount in value comparing with the value of Q_{V}. According to Fig. 7(e), there is a remarkable effect on the intravasations by the anti-angiogenesis treatments. Q_{t}^{-} in the first three study goups (AGF&AS, AGF&ES, AGF&AS&ES:10) decreases 36%, 42%, and 94%, respectively, and no intravasation appears in the last two groups (AGF&AS&ES:6, AGF&AS&ES:4), which may reduce the chances of metastasis of various growth factors or even tumor cell through the intravasation inside the tumor.

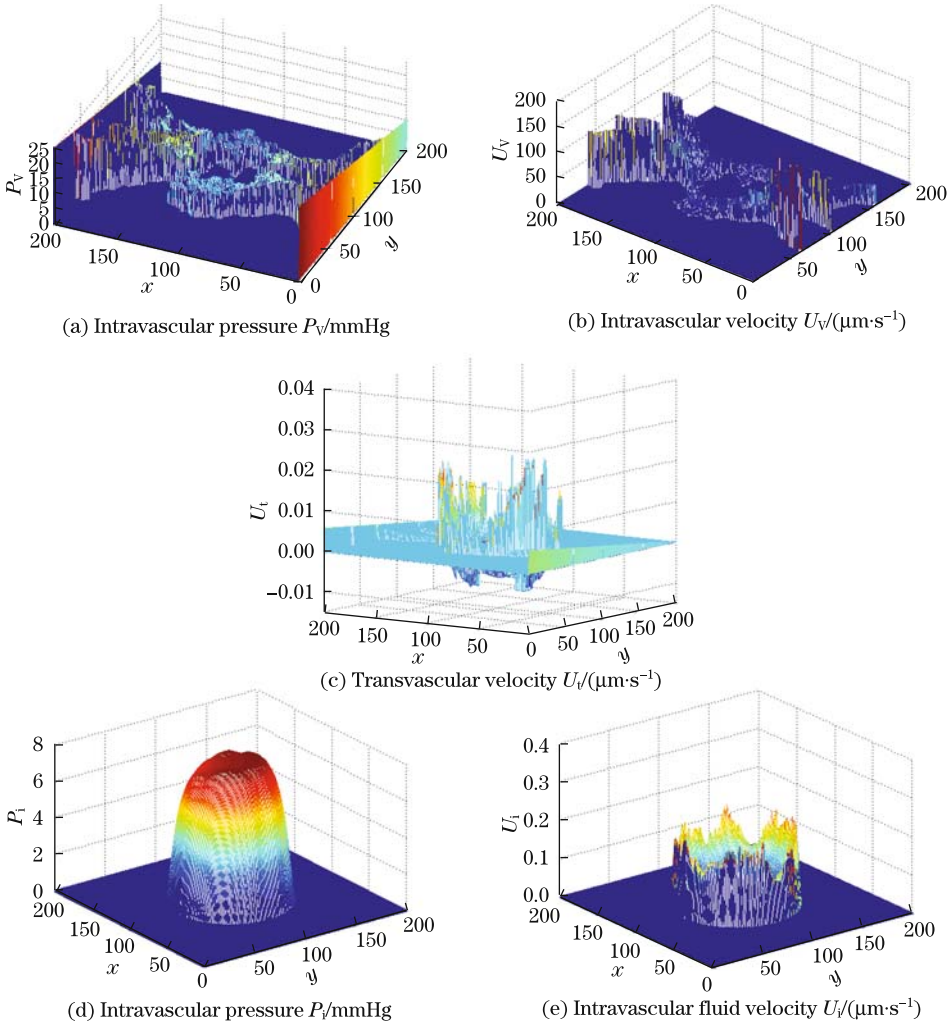

(a) Intravascular pressure P_{V}/mmHg

(b) Intravascular velocity U_{V}/(μm·s^{-1})

(c) Transvascular velocity U_{t}/(μm·s^{-1})

(d) Intravascular pressure P_{i}/mmHg

(e) Intravascular fluid velocity U_{i}/(μm·s^{-1})

Fig. 6 Flow simulation results of the control group AGF (the netowrk in Fig. 4(a))

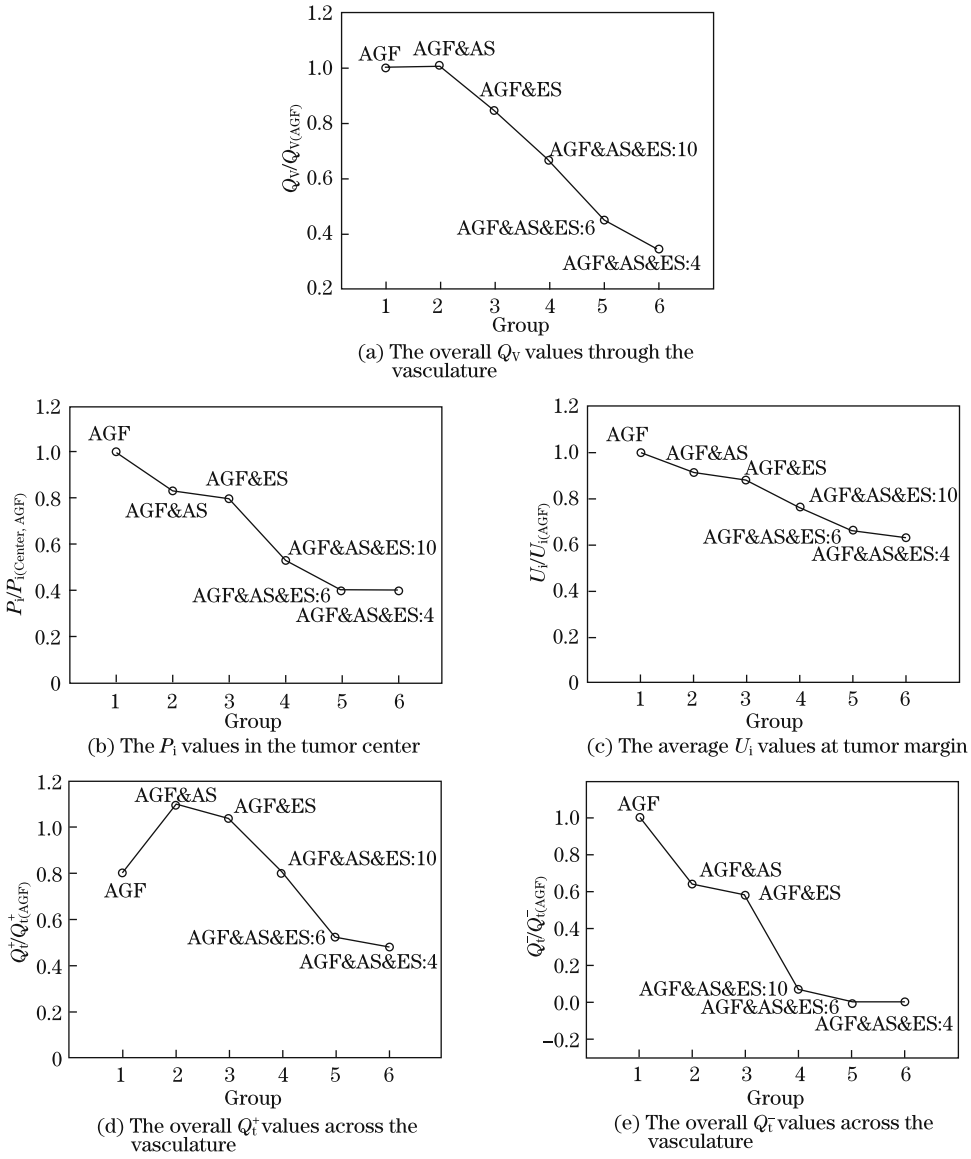

Fig. 7 Comparisons of the flow values

4 Conclusions

The effects of anti-angiogenesis treatment by angiostatin and endostatin on normalization of tumor microvasculature and microenvironment are investigated. The results in this paper suggest that these tumor vessels are "normalized" by anti-angiogenesis treatment and the resultant network is more efficient: (i) the proliferation, growth, and branching of neo-vessels are effectively inhibited, and the extent of vascularization in tumors is accordingly reduced. (ii) based on the anti-angiogenic vasculature, the overall blood perfusion inside of tumor is declined, the plateau of tumor IFP is relieved, the interstitial fluid oozing out from the tumor periphery into the surrounding normal tissue is reduced, the reduction of overall extravasation

across vasculature to tumor interstium is much less than the decreased overall blood perfusion, due to the decline of IFP, the intravasation is remarkablely effected by the change, and in some cases, no intravasation flow appears.

References

[1] Jain, R. K., Tong, R. T., and Munn, L. L. Effect of vascular normalization by antiangiogenic therapy on interstitial hypertension, peritumor edema, and lymphatic metastasis: insights from a mathematical model. *Cancer Research*, **67**(6), 2729–2735 (2007)

[2] Fukumura, D. and Jain, R. K. Tumor microvasculature and microenvironment: targets for anti-angiogenesis and normalization. *Microvascular Research*, **74**, 72–84 (2007)

[3] Huber, P. E., Bischof, M., Jenne, J., Heiland, S., Peschke, P., Saffrich, R., Gröne, H. J., Debus, J., Lipson, K. E., and Abdollahi, A. Trimodal cancer treatment: beneficial effects of combined antiangiogenesis, radiation, and chemotherapy. *Cancer Research*, **65**(9), 3643–3655 (2005)

[4] Tong, R. T., Boucher, Y., Kozin, S. V., Winkler, F., Hicklin, D. J., and Jain, R. K. Vascular normalization by vascular endothelial growth factor receptor 2 blockade induces a pressure gradient across the vasculature and improves drug penetration in tumors. *Cancer Research*, **64**(11), 3731–3736 (2004)

[5] Willett, C. G., Boucher, Y., di Tomaso, E., Duda, D. G., Munn, L. L., Tong, R. T., Chung, D. C., Sahani, D. V., Kalva, S. P., Kozin, S. V., Mino, M., Cohen, K. S., Scadden, D. T., Hartford, A. C., Fischman, A. J., Clark, J. W., Ryan, D. P., Zhu, A. X., Blaszkowsky, L. S., Chen, H. X., Shellito, P. C., Lauwers, G. Y., and Jain, R. K. Direct evidence that the anti-VEGF antibody Bevacizumab has anti-vascular effects in human rectal cancer. *Nat. Med.*, **10**, 145–147 (2004)

[6] Willett, C. G., Boucher, Y., Duda, D. G., di Tomaso, E., Munn, L. L., Tong, R. T., Kozin, S. V., Petit, L., Jain, R. K., Chung, D. C., Sahani, D. V., Kalva, S. P., Cohen, K. S., Scadden, D. T., Fischman, A. J., Clark, J. W., Ryan, D. P., Zhu, A. X., Blaszkowsky, L. S., Shellito, P. C., Mino-Kenudson, M., and Lauwers, G. Y. Surrogate markers for antiangiogenic therapy and dose-limiting toxicities for Bevacizumab with radiation and chemotherapy: continued experience of a phase I trial in rectal cancer patients. *J. Clin. Oncol.*, **23**, 8136–8139 (2005)

[7] O'Reilly, M. S., Holmgren, L., Shing, Y., Chen, C., Rosenthal, R. A., Moses, M., Lane, W. S., Cao, Y., Sage, E. H., and Folkman, J. Angiostatin: a novel angiogenesis inhibitor that mediates the suppression of metastases by a Lewis lung carcinoma. *Cell*, **79**, 315–328 (1994)

[8] O'Reilly, M. S., Boehm, T., Shing, Y., Fukai, N., Vasios, G., Lane, W. S., Flynn, E., Birkhead, J. R., Olsen, B. R., and Folkman, J. Endostatin: an endogenous inhibitor of angiogenesis and tumor growth. *Cell*, **88**, 277–285 (1997)

[9] Tee, D. and Distefano, J., III. Simulation of tumor-induced angiogenesis and its response to anti-angiogenic drug treatment: mode of drug delivery and clearance rate dependencies. *J. Cancer Res. Clin. Oncol.*, **130**, 15–24 (2004)

[10] Zhao, G. P., Gao, H., Wu, J., Xu, S. X., Collins, M. W., Long, Q., König, C. S., and Padhani, A. R. 2D numerical simulation of effect anti-angiogenic factors angiostatin and endostatin on tumor-induced angiogenesis (in Chinese). *J. Med. Biomech.*, **21**(4), 272–279 (2006)

[11] Anderson, A. R. A. and Chaplain, M. A. J. Continuous and discrete mathematical models of tumor-induced angiogenesis. *Bull. Math. Biol.*, **60**, 857–900 (1998)

[12] Wu, J., Xu, S. X., Long, Q., Collins, M. W., König, C. S., Zhao, G., Jiang, Y., and Padhani, A. R. Coupled modeling of blood perfusion in intravascular, interstitial spaces in tumor microvasculature. *J. Biomech.*, **41**, 996–1004 (2008)

[13] Wu, J., Long, Q., Xu, S. X., and Padhani, A. R. Study of tumor blood perfusion and its variation due to vascular normalization by anti-angiogenic therapy based on 3D angiogenic microvasculature. *J. Biomech.*, **42**, 712–721 (2009)

[14] Baxter, L. T. and Jain, R. K. Transport of fluid and macromolecules in tumors. II. Role of heterogeneous perfusion and lymphatics. *Microvascular Research*, **40**, 246–263 (1990)

[15] Wan, R. Dynamics of lymphatic return (in Chinese). *Biology Teaching*, **9**, 32 (1993)

[16] Netti, P. A., Roberge, S., Boucher, Y., Baxter, L. T., and Jain, R. K. Effect of transvascular fluid exchange on pressure-flow relationship in tumors: a proposed mechanism for tumor blood flow heterogeneity. *Microvascular Research*, **52**, 27–46 (1996)

[17] Pries, A. R., Secomb, T. W., Gessner, T., Sperandio, M. B., Gross, J. F., and Gaehtgens, P. Resistance to blood flow in microvessels in vivo. *Circulation Research*, **75**, 904–915 (1994)

[18] Pries, A. R. and Secomb, T. W. Microvascular blood viscosity in vivo and the endothelial surface layer. *Am. J. Physiol. Heart Circ. Physiol.*, **289**, H2657–H2664 (2005)

[19] Eriksson, K., Magnusson, P., Dixelius, J., Claesson-Welsh, L., and Cross, M. J. Angiostatin and endostatin inhibit endothelial cell migration in response to FGF and VEGF without interfering with specific intracellular signal transduction pathways. *FEBS Letters*, **536**, 19–24 (2003)

[20] Herbst, R. S., Mullani, N. A., Davis, D. W., Hess, K. R., McConkey, D. J., Charnsangavej, C., O'Reilly, M. S., Kim, H. W., Baker, C., Roach, J., Ellis, L. M., Rashid, A., Pluda, J., Bucana, C., Madden, T. L., Tran, H. T., and Abbruzzese, J. L. Development of biologic markers of response and assessment of antiangiogenic activity in a clinical trial of human recombinant endostatin. *J. Clin. Oncol.*, **20**, 3804–3814 (2002)